NANO LETTERS

Letter

pubs.acs.org/NanoLett

Giant Nanocrystal Quantum Dots: Stable Down-Conversion Phosphors that Exploit a Large Stokes Shift and Efficient Shell-to-Core Energy Relaxation

Janardan Kundu, Yagnaseni Ghosh, Allison M. Dennis, Han Htoon, and Jennifer A. Hollingsworth*

Materials Physics and Applications Division, Center for Integrated Nanotechnologies, Los Alamos National Laboratory, Los Alamos, New Mexico 87545, United States

Supporting Information

ABSTRACT: A new class of nanocrystal quantum dot (NQD), the "giant" NQD (g-NQD), was investigated for its potential to address outstanding issues associated with the use of NQDs as down-conversion phosphors in light-emitting devices, namely, insufficient chemical/photostability and extensive self-reabsorption when packed in high densities or in thick films. Here, we demonstrate that g-NQDs afford significantly enhanced operational stability compared to their conventional NQD counterparts and minimal self-reabsorption losses. The latter results from a characteristic large Stokes shift (>100 nm; >0.39 eV), which itself is a manifestation of the internal structure of these uniquely thick-shelled NQDs. In carefully prepared g-NQDs, light absorption occurs predominantly in the shell but emission occurs exclusively from the core. We directly compare for the first time the processes of shell→core energy relaxation and core→core energy transfer by evaluating CdS→CdSe down-conversion of blue→red light in g-NQDs and in a comparable mixed-NQD (CdSe and CdS) thin film, revealing that the internal energy relaxation process affords a more efficient and color-pure conversion of blue to red light compared to energy transfer. Lastly, we demonstrate the facile fabrication of white-light devices with correlated color temperature tuned from ∼3200 to 5800 K.

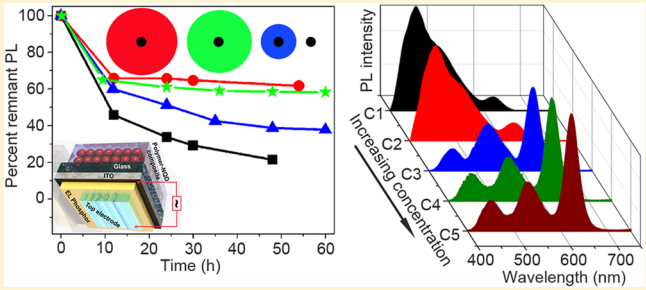

KEYWORDS: *Giant nanocrystal quantum dot (g-NQD), stable red phosphor, self-reabsorption, Stokes shift, down-conversion light-emitting device*

Artificial lighting consumes ∼20% of electrical energy produced.[1] While fluorescent and high-intensity discharge lamp replacements for incandescent bulbs have afforded significant gains in lighting efficiencies, even more efficient options are sought to further reduce the substantial energy costs associated with artificial lighting. A key emerging alternative lighting technology is solid-state lighting (SSL), which relies on semiconductor light-emitting diode (LED) devices to directly convert electricity to light. To realize white-light emission, appropriate mixing of component colors (e.g., blue, green, yellow, and/or red) is required. This is achieved by either using differently colored "primary" semiconductor LEDs in conjunction with one another, or by including "secondary" wavelength-converting materials to alter the color spectrum of a primary source LED.[2] In many respects, the latter approach is the simplest to implement, requiring electronic control of as few as one driving LED. Further, the former approach continues to suffer from inadequate efficiencies of green/amber sources and so-called "current droop."[3] Thus, as a result of the practical utility of phosphor-converted LEDs, research into new color-converting phosphor technologies is an ongoing and active research area driving the development of improved SSL technologies.[4]

Most commonly, color-converting phosphors comprise rare earth dopant ions embedded in a host matrix (e.g., garnets, sulfides, (oxy)nitrides). The well-known Ce^{3+} doped $Y_3Al_5O_{12}$ (YAG:Ce) achieves high quantum efficiencies (∼90%) but affords broad yellow emission that must be combined with other phosphors to realize high color rendering.[5] Alternative or complementary rare earth phosphors can be limited by lower emission efficiencies or insufficient chemical/photostabilities and often exhibit nonideal excitation (narrow or weak bands) or emission (broad, especially contributing to deep-red emission where eye sensitivity is poor) profiles.[2] Also, although Eu^{2+} and Ce^{3+} ions offer relatively short emission decay times and, thereby, minimal saturation at high photon fluxes, other rare earth ions and alternative dopants (e.g., Mn^{2+}) are characterized by nonideal, long lifetimes.[2,4,5] For these reasons, new color-shifting phosphors are required to meet the needs of high-efficiency, robust SSL technologies.

Nanocrystal quantum dots (NQDs) promise advantages as phosphors in SSL. NQDs are characterized by efficient (large

Received: March 2, 2012
Revised: May 3, 2012
Published: May 8, 2012

absorption cross sections) and broadband absorption, as well as efficient and narrowband (<35 nm) emission.[6] Significantly, NQD emission color is easily tunable by manipulating particle size within the quantum confinement regime (e.g., <10 nm for II−VI NQDs).[2,6] And, as nanoscale phosphors, NQDs offer the added advantage, compared to conventional rare earth micrometer-scale phosphors, of negligible scattering for enhanced beam collimation, minimal backscatter to the source LED, and minimal internal scattering losses.[2] These enabling properties have led to realization of proof-of-concept demonstrations of NQDs as color-converting phosphors in single-color and white-light emitting devices.[7−15] Overall, however, long-term chemical/photostability under operating conditions[16,17] is also a question for NQDs, as is optical performance in the solid-state, given that conventional NQDs rely on a stabilizing and passivating organic ligand layer to achieve high quantum yields (QYs) in emission. This ligand layer is susceptible to damage or degradation during device processing or operation. In addition, a key issue limiting NQD utility for down-conversion phosphor applications is the small Stokes shift (minimal spectral separation between absorption onset and emission) characteristic of these nanomaterials, which results in strong self-reabsorption (or yellow/green absorption by red-emitting NQDs) that is anticipated to have a detrimental impact on solid-state efficiencies as NQD packing density or loading fraction is increased.[2,4,15]

We recently reported the synthesis and characterization of thick-shell or "giant" CdSe/CdS core/shell NQDs (g-NQDs).[18−22] g-NQDs are prepared by overcoating a CdSe core (typically 3−4 nm diameter) with many monolayers (~11−20 MLs) of higher bandgap CdS, resulting in ~10−20 nm particles.[18,19,22] CdSe/CdS g-NQDs are characterized by a quasi-type II electronic structure, wherein the hole remains confined within the core while the electronic wave function delocalizes into the shell.[23] Significantly, they exhibit many of the enabling characteristics of conventional NQDs but with suppressed single-dot-level blinking behavior[18,19] and suppressed nonradiative Auger recombination,[20] as well as unparalleled chemical/photostability and a large Stokes shift.[18,19] We have also shown that compared to their thinner shell counterparts, g-NQDs exhibit enhanced solid-state performance as direct-charge-injection light-emitting layers.[22] Here, we explore the utility of g-NQDs as novel down-conversion phosphors. We reveal enhanced operational stability and suppressed self-reabsorption and green absorption in the case of red-emitting g-NQDs. Specifically, we deposit g-NQD layers onto a blue-emitting device and assess their ability to convert the higher energy light into red emission. We do so as a function of g-NQD concentration, and we compare to core-only and conventional core/shell NQDs. We also directly compare the down-conversion process in g-NQDs, which is dominated by shell→core (CdS→CdSe) energy relaxation, with core→core energy transfer in a mixed CdSe and CdS NQD system, revealing a clear advantage of internal energy conversion processes over external, proximity-driven energy transfer. Lastly, we demonstrate facile incorporation of red g-NQDs into white-light-emitting devices that span a range of cool to warm color temperatures.

As our "test-bed" device, we fabricated an alternating-current (ac) electroluminescent (EL) device[10,11] using a commercially available, EL powder phosphor (Cu/Cl doped ZnS, Global Tungsten & Powders Corp.) that emits in the blue (λ_{max} ~445 nm). The powder was dispersed in a transparent, insulating binder and deposited as a uniform, pinhole-free phosphor layer using a doctor blading technique onto surface-treated indium tin oxide (ITO) coated glass (see Supporting Information for a detailed experimental description). ITO served as a bottom electrode, and conducting Cu tape (3M) was used as a top electrode (Figure 1a). The active device area is determined by the overlap between the top electrode and the bottom ITO layer.[10,11] We applied a layer of NQDs encapsulated in a poly(lauryl methacrylate) (PLMA) matrix onto the back side of the device (Figure 1b). PLMA was chosen as the NQD matrix as it has been shown to afford minimal losses in emission efficiency otherwise resulting from the transfer of NQDs from the solution phase to the solid state.[24] This consideration is most relevant for core-only and conventional core/shell NQDs, whose emission in solid films is more deleteriously affected than that of g-NQDs.[22] The EL phosphor was electrically excited using a high frequency (31 kHz) AC voltage (~350 V_{rms}). All NQDs were fabricated following modified or newly developed procedures (Supporting Information).[18,19,25] With the exception of the PLMA matrix, no special "packaging" of the devices was done, and devices were tested in ambient conditions using a fluorimeter (Horiba Jobin Yvon Nanolog) to record EL and photoluminescence (PL) spectra or a spectroradiometer (Konica Minolta CS-2000) to assess luminance.

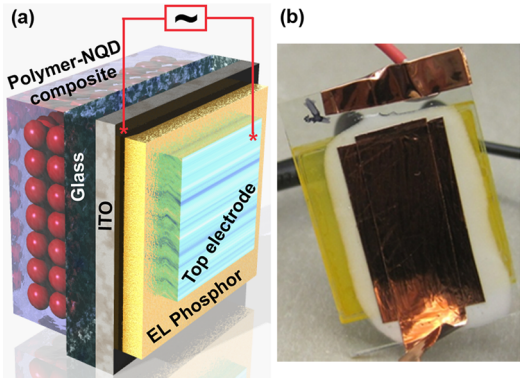

Figure 1. (a) Cross-sectional view of device schematic. (b) fabricated g-NQD active device with yellow g-NQD layer on glass, white phosphor material on ITO, and conducting Cu tape on the phosphor material as the top electrode.

The ability of CdSe/CdS g-NQDs to serve as effective EL down-conversion phosphors is revealed in their unusual absorption profile (Figure 2a). g-NQDs afford efficient absorption in the blue spectral region (<500 nm), but minimally absorb above the band edge of the shell material, CdS (512 nm). Absorption in these ultrathick shell systems is dominated by the shell, which comprises >80% of the total particle volume. For this reason, they readily down-convert blue EL phosphor emission to red PL (~620 nm here), while leaving green components of the EL spectrum relatively less affected (Figure 2b). This unequal effect on blue and green light is evident in Figure 2b, where down-conversion is shown for increasing concentrations of g-NQD phosphors. Increasing g-NQD concentrations result in dramatic reductions in blue emission, initially the dominant component in the EL spectrum, but leave a slightly red-shifted green component intact, such that it dominates the EL contribution to the total

dx.doi.org/10.1021/nl3008659 | Nano Lett. 2012, 12, 3031−3037

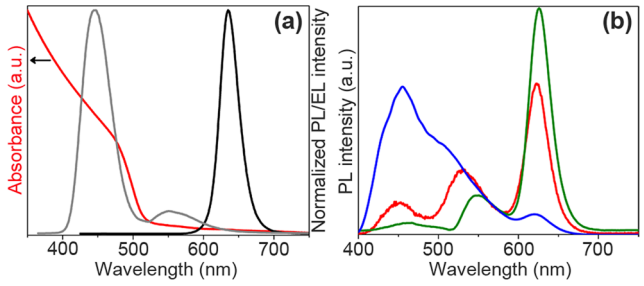

Figure 2. Optical down-conversion. (a) Electroluminescence spectrum of phosphor (gray) under ac bias voltage, PL spectrum (black) and absorption spectrum (red) of g-NQDs. (b) Emission spectra of devices with increasing concentrations of red-emitting g-NQDs under constant ac bias voltage (concentrations increasing from blue to red to green).

device emission profile at high g-NQD concentrations. At the same time, g-NQD red emission effectively "replaces" blue EL.

The extent to which red PL replaces blue EL was assessed in terms of "down-conversion efficiency." NQD down-conversion efficiency can be described as the ratio of NQD PL (in watts) to the phosphor EL (in watts).[11] We obtained a down-conversion efficiency of 22% for the highest g-NQD concentration device (Figure 2b, green trace), which was fabricated using CdSe/CdS g-NQDs comprising 16 monolayers of CdS shell (one monolayer = 0.3375 nm). This conversion efficiency is relatively high compared to previous reports describing NQD down-conversion devices (e.g., 12%)[11] but consistent with the fact that g-NQD solution-phase behavior (here, g-NQD solution QYs, are ~45%) is better retained in the solid state compared to that for conventional NQDs, whose performance in the solid state suffers from a range of effects, including damage to the protective ligand layer and NQD-to-NQD energy transfer processes.[22] In addition, we are employing a near-ideal polymer matrix (PLMA) to facilitate formation of uniform, optically transparent NQD films. This polymer is known to reduce liquid-to-solid-state emission losses.[24] For these reasons, we believe that the primary losses in the down-conversion process derive from our clearly unoptimized device geometry, where the intervening glass slide that separates the EL material from the NQD phosphor layer could result in substantial waveguiding losses (though transmission at 450 nm is ~100% for standard glass). Spectral purity for this device, defined as the fraction of the device emission spectrum contributed by red NQD PL, was determined to be 0.84. The deviation from a value of 1.0 (or 100% color purity) is due primarily to the remaining green EL component rather than from unconverted blue EL, as most of the blue EL component was quenched (Figure 2b). Lastly, a reasonably high luminance (brightness) of ~30 Cd/m^2 (under 350 V_{rms} at 31 kHz AC bias) was observed and did not diminish when retested after storage in air for several months.

The fact that g-NQDs do not quench green emission is important for their potential application as red phosphors in white-light-emitting down-conversion devices that rely on a combination of a blue EL source and green and red emitters. Elimination of unwanted green absorption simplifies fabrication of white-emitting devices as we demonstrate below. In addition, the significant spectral separation between g-NQD PL emission and the primary absorption onset of ~120 nm (620 nm − 500 nm) implies a large effective Stokes shift and, thereby, minimal self-reabsorption. In contrast, core-only NQDs and conventional core/shell NQDs are characterized by a much smaller Stokes shift of ~20 nm, as efficient absorption initiates above 600 nm (Figure 3a). In the context of their application to solid-state lighting, the small Stokes shift of standard NQDs has been described as the "most fundamental concern about QDs" as this feature results in self-reabsorption, which "red shifts and reduces the efficiency of light emission."[2]

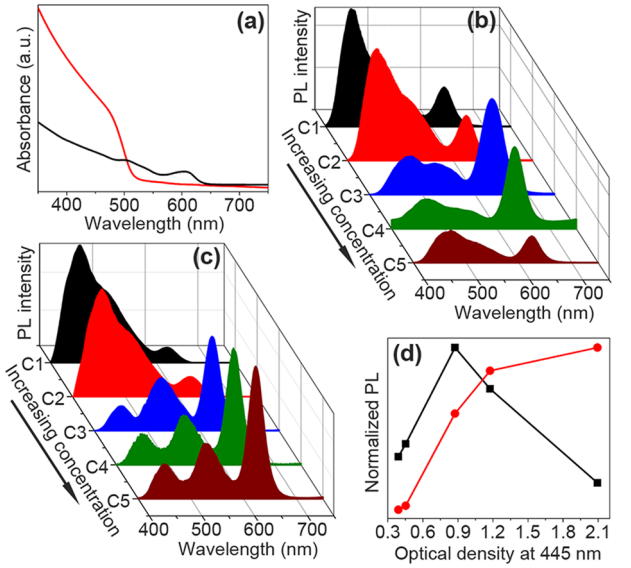

Figure 3. Effect of self-reabsorption on emission: (a) Absorption profile of g-NQD (red solid line) and core NQD (black solid trace). (b) Emission spectra of core-only devices for increasing core-NQD concentrations. (c) Emission spectra of g-NQD devices for increasing g-NQD concentrations. (d) Normalized PL intensity for the red spectral component as a function of NQD optical density (at 445 nm) for core-only devices (black) and g-NQD devices (red).

As a practical demonstration of the utility of the larger g-NQD Stokes shift, we compared down-conversion device performance for red-emitting core-only and g-NQD devices of increasing (and comparable) optical densities (ODs) at 445 nm (blue EL maximum) (Figure 3b–d), where ODs were controlled by changing NQD concentrations in the PLMA films while maintaining film thicknesses (Supporting Information). In both cases, red PL intensity initially increased with increasing NQD OD. However, in the case of core-only CdSe NQDs (5 nm diameter) the highest NQD concentrations (ODs) exhibited reduced emission compared to their lower concentration counterparts (Figure 3b,d). In contrast, red emission from g-NQD devices (here: 11-monolayer thick CdS shell) continued to increase as a function of NQD OD (Figure 3c,d). Our results for the core-only NQD devices are consistent with an earlier study employing conventional core/shell NQDs in which it was shown that device down-conversion efficiency decreased as the number dot layers was increased.[11] It is, therefore, noteworthy that we see the opposite trend in the case of g-NQDs. It is also worth noting that at the highest core-only NQD concentrations, green EL is also quenched, which, again, is not observed for g-NQD phosphors. Thus, g-NQDs afford an enhanced opportunity to "concentration tune" device light output without deleterious self-reabsorption or green absorption.

The large g-NQD Stokes shift results from the fact that emission originates from the CdSe core, while most of the

dx.doi.org/10.1021/nl3008659 | Nano Lett. 2012, 12, 3031−3037

absorption cross section derives from the CdS shell. In this case, shell excitations relax nonradiatively into the lower-energy core-emitting state. Because of structural similarities with epitaxial quantum dot-in-quantum well systems,[18] in which quantum dot exciton capture is known to be efficient,[26] we anticipate that g-NQD shell→core energy relaxation is similarly effective. Nevertheless, a question remains as to whether it is necessary that the absorbing CdS and emitting CdSe components interact via a single core/shell construct, or whether these components can be equally effective when present as distinct structures. For example, in the case of an intimate mixture of CdSe and CdS NQDs, higher energy excitons originating in the CdS component may still be converted into CdSe red emission, though by a different mechanism. In such a case, CdS NQDs would transfer excitation energy to nearby CdSe NQDs by way of nonradiative dipole−dipole mediated energy transfer (ET), where transfer efficiency strongly depends on several experimental conditions, including CdSe/CdS dot/dot spatial separations, spectral overlap integral between donor emission and acceptor absorption, donor QY in emission, and acceptor/donor ratio.[27−29] In this way, an ET-mediated process might constitute a viable alternative excitation mechanism, and mixed films of CdSe and CdS NQDs might, therefore, afford an alternative down-conversion phosphor with advantages of synthetic simplicity compared to the relatively more elaborate CdSe/CdS g-NQD.

To test this hypothesis, we prepared a mixed-dot film comprising CdSe and CdS NQDs (Supporting Information Figure S3) that "mimics" g-NQDs with respect to CdSe/CdS volume ratio, CdS surface chemistry, and red-emission QY. Specifically, we prepared a mixture of CdSe and CdS NQDs that was characterized by the same blue/red OD ratio as the g-NQDs, that is, OD_{447}/OD_{610} = ~5.85. Within this constraining condition, the total number of NQDs was varied to achieve an OD at the excitation wavelength (450 nm) that was equivalent to a comparison g-NQD film (Figure 4a). The resulting mixed-NQD film was characterized by a CdSe/CdS dot/dot ratio of 1:9, which is similar to the analogous g-NQD CdSe/CdS volume ratio (note: dot number and volume ratios are approximately comparable here, as the CdSe and CdS NQD cores were of similar size − 4.9 and 5.2 nm, respectively). Further, the CdSe NQD cores were synthesized to provide emission near that of the g-NQDs (λ_{em} = 610 nm), and g-NQDs were chosen that had a similar QY as the core-only CdSe NQDs (30% compared to 28%, respectively).

Significantly, to minimize CdSe/CdS dot/dot separation and enhance ET efficiency,[27,28] we prepared the films by drop-casting from NQD solutions in hexane/octane (9:1) mixtures, rather than as PLMA-dot composites. In this way, we ensured close-packing of the mixed-system NQDs, such that nearest-neighbor NQDs are separated by only their ligand layer (~1 nm).[27,28,30] Resulting NQD/NQD center-to-center distances equal the donor-NQD radius plus the acceptor-NQD radius plus the separation induced by the ligand layer,[27,28,30] or 2.45 nm (CdS radius) plus 2.60 nm (CdSe radius) plus ~1 nm for our system (~6 nm total). This distance is comparable to previously reported NQD/NQD donor−acceptor distances and critical ET distances (the distance at which the ET transfer rate equals the rate of other donor de-excitation pathways), that is, ~5−6 nm and ~5 nm, respectively.[27,28] Further, given that the CdS and CdSe NQDs were similar in size (see above), we minimized any tendency for size-segregation effects and

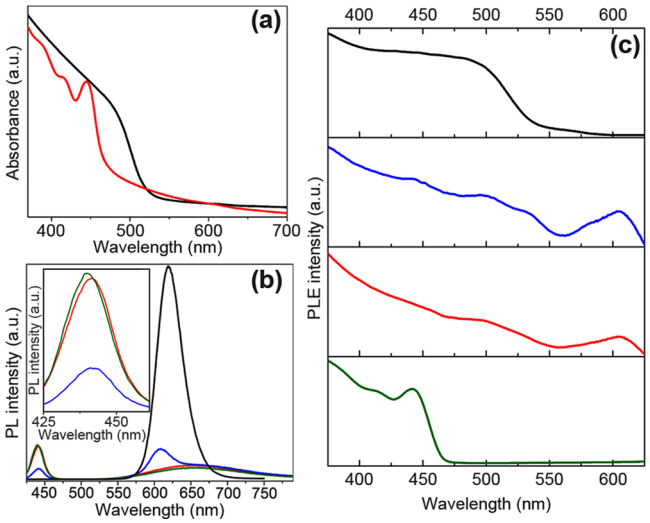

Figure 4. (a) Absorbance spectra of g-NQD (black) and mixed-core (red) films at "matching" concentrations. (b) PL emission spectra of g-NQD film (black), CdS-only NQD film (green), mixed CdSe-CdS film with CdSe/CdS ratio (1:9) matched to g-NQD system (red), mixed CdSe/CdS film with CdSe/CdS ratio enhanced in acceptor (4:9) (blue). All films were excited at 405 nm. Inset magnifies CdS emission region to highlight decreases in CdS donor PL intensity resulting from addition of CdSe acceptor NQDs to a CdS film. (c) PLE spectra of g-NQD film at 620 nm (black trace); mixed-core system with "excess" CdSe acceptors added at 620 nm (blue trace); CdSe film at 650 nm (red trace), and CdS film at 610 nm (green trace).

promoted good CdS/CdSe dot/dot mixing. In addition to NQD close-packing, the excellent spectral overlap between CdS emission and CdSe absorption [compare Figure 4c CdSe photoluminescence excitation, PLE, spectrum (red trace) with 4b CdS PL spectrum (green trace)] supports ET from CdS to CdSe. We note, however, that two features of our analogue mixed CdSe/CdS system were not optimized for efficient ET. Namely, the small acceptor/donor ratio, determined by the CdSe/CdS ratio in our g-NQDs, does not favor ET.[29] Furthermore, the relatively low QY of our donor CdS NQDs (~17% solution-phase QY determined by comparison to reference dye, Coumarin 460, which was further diminished in the solid-state as evidenced by formation of significant red trap emission in the films, see below) is not ideal for efficient ET.[27,28] However, we chose not to augment the CdS NQD QY by, for example, adding a protective, passivating ZnS shell, as our g-NQDs are CdS-terminated and, therefore, not themselves protected or passivated by a higher-bandgap shell, allowing us to retain parity in terms of surface-chemistry.

Results for a typical mixed-NQD/g-NQD comparison are shown in Figure 4b. In contrast with the g-NQD film, which shows exclusively narrow-band excitonic CdSe emission, the mixed-NQD film emission is dominated by CdS excitonic and trap emission, where the latter results in a broad red "peak" that dwarfs any contribution from excitonic CdSe NQD emission. Overall, film emission intensity is significantly weaker for the mixed system compared to the g-NQD system. By comparing donor CdS NQD PL intensity without (I_D) and with (I_{DA}) acceptor CdSe NQDs, we obtain low ET efficiencies of ~5% according to the relationship: ET efficiency = $1 - I_{DA}/I_D$.[31] ET in this mixed-NQD film likely suffers from both the poor QY of the donor CdS NQDs and the low acceptor/donor ratio. Indeed, we show that by increasing the amount of CdSe in the

dx.doi.org/10.1021/nl3008659 | Nano Lett. 2012, 12, 3031−3037

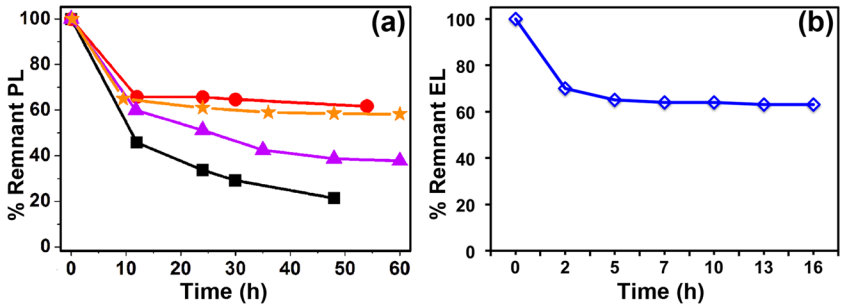

Figure 5. (a) Temporal device stability revealed by percent remnant PL intensity as a function of continuous biasing time for various devices: core only (black), 4-shell CdSe/CdS NQDs (purple), 11-shell CdSe/CdS g-NQDs (orange), and 16-shell CdSe/CdS g-NQDs (red). (b) Temporal device stability for a phosphor-only device (blue).

films (acceptor/donor ratio of 4:9), more of the CdS NQD emission is successfully transferred to CdSe, as indicated by decreased CdS emission intensity compared to either the CdS-only film or the mixed-NQD films with CdSe/CdS ratios matched to the g-NQD system (Figure 4b and inset, blue traces). Here, the sharp excitonic CdSe emission peak is evident in the film PL spectrum (Figure 4b, blue trace). Nevertheless, even in this case where we have incorporated "excess" (compared to the CdSe contribution in g-NQDs) CdSe NQDs into the mixed-NQD film, CdSe emission remains an order-of-magnitude weaker than that observed for the comparison g-NQD film (Figure 4b, blue compared to black traces).

The inability of the mixed-NQD system to afford CdS→CdSe excitation comparable to the g-NQD system is also evident in PLE data (Figure 4c). g-NQD PLE clearly follows the smooth onset of bulklike CdS absorption, while that for a mixed system (with excess CdSe acceptors) more closely resembles CdSe NQD-only PLE with some contribution from CdS NQD absorption. ET efficiency in the mixed CdS/CdSe NQD system could be significantly enhanced by further adjustments to the acceptor/donor ratio and in improvements to the donor CdS NQD QY. However, the comparison to the g-NQD core/shell system would then be less direct. Furthermore, NQD close-packing could be further optimized by employing alternative film-formation techniques, such as Langmuir−Blodgett (LB) approaches,[32] as well as by replacement of the existing surface ligands with more compact ligands, but LB is not an obvious choice for large-area, low-cost processing that is desirable for SSL, and ligand replacement can deleteriously impact emission efficiencies in the case of conventional NQDs. Thus, although g-NQDs entail a relatively more complex internal heterostructure, they conveniently "tolerate" what is effectively a small acceptor/donor ratio, as well as the lack of passivation of the CdS surface by further shelling. Neither seems to impede the down-conversion of higher energy CdS excitations into red CdSe emission. Significantly, the absorbing and emitting species are effectively intimately "mixed" by way of the core/shell interface.

Lastly, even in the case of an optimized mixed-NQD ET system, the ET process is likely universally less efficient compared to shell→core energy relaxation. Specifically, although NQD-NQD ET rates as fast as 38 ps have been predicted,[32] to the best of our knowledge the fastest observed NQD-NQD ET rate is 50 ps, and this result was restricted to a carefully prepared NQD monolayer film.[32] Most reported NQD-NQD rates are substantially longer (700−10 000 ps).[27,28] In contrast, studies of self-assembled quantum dots (SAQD), the most structurally equivalent QD to our g-NQDs, have shown that carriers generated in barrier layers of SAQDs can be captured at the rate of 2−30 ps.[33,34] It is likely that in our more confined g-NQDs, this capture rate is even faster. Indeed, the essentially instantaneous rise of g-NQD PL signal observed in time-resolved PL (TR-PL) measurements[20] shows that the carrier capture time is shorter than the time-response of the TR-PL system, which is 50 ps, providing an upper limit to the shell→core energy relaxation time of <50 ps. Thus, this process appears generally superior to NQD-NQD ET as a down-conversion mechanism for NQD-based phosphor applications.

Beyond efficiency, compared to core-only or conventional core/shell NQDs, g-NQDs are less susceptible to photobleaching and reductions in PL resulting from modifications to NQD ligand coatings.[18,19] To assess whether this enhanced NQD stability translates into enhanced device stability, we studied the long-term operational performance of these devices under continuous ac bias voltage. Down-converted red-PL intensities were followed for more than 50 h. g-NQD devices (11-monolayer and 16-monolayer CdS shells) were compared to core-only and thinner-shell (4-monolayer CdS shell) core/shell NQD devices (Figure 5a). In all cases, an initial loss in PL intensity was observed that we attribute primarily to a decline in the performance of the blue EL phosphor, which exhibited an initial efficiency drop then stabilized over time (Figure 5b). This behavior is thought to result from generic "aging/stabilization" effects.[5,35] Significantly, the magnitude of the initial decline in g-NQD device performance was found to be similar to that of the source blue EL phosphor, that is, after ∼10 h of operation, the percent remnant PL or EL was ∼65%. Following this loss, both g-NQD devices remained stable over the ∼50 h observation time. In contrast, the PL intensity for core-only and thinner-shell devices continued to drop, never stabilizing. This relative instability cannot be attributed to a decline in the blue phosphor performance alone, but, rather, must also originate from the degradation (presumably photo-oxidative) of the NQD emitters. Note: the fact that the core-only device performed at even ∼25% of its original intensity after 50 h is likely attributable to the protective PLMA matrix. Nevertheless, thick CdS shells clearly enhance CdSe/CdS device stability beyond that afforded by even polymer encapsulation.

Finally, we show that red-emitting CdSe/CdS g-NQDs can be combined with green-emitting NQDs and the blue EL phosphor to produce white light. In general, due to their narrow and particle-size-tunable emission bands, NQD emitters can facilitate the fabrication of white-emitting devices with high correlated-color-temperatures (CCTs), while maintaining the

dx.doi.org/10.1021/nl3008659 | Nano Lett. 2012, 12, 3031−3037

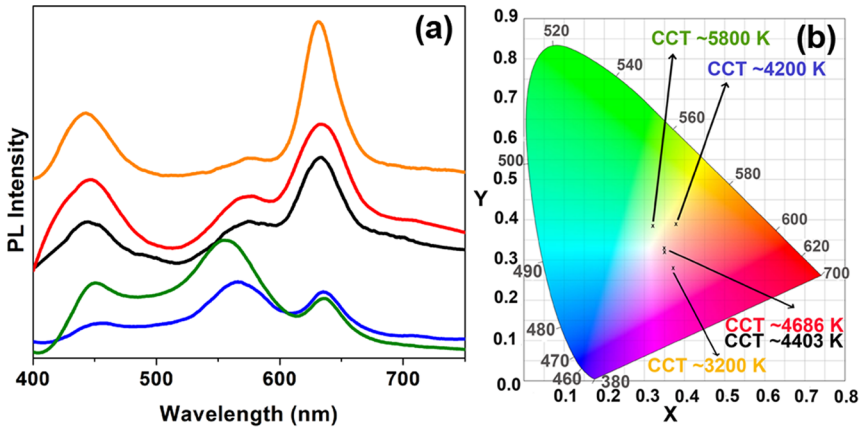

Figure 6. White-light generation by additive color mixing utilizing red g-NQDs and green NQDs as phosphor materials in AC down-conversion devices: (a) PL emission spectra of various devices with different CIE coordinates and CCT (K): orange trace (0.37, 0.28; 3200 K), black trace (0.35, 0.32; 4403 K), red trace (0.35, 0.33; 4686 K), green trace (0.32, 0.38; 5800 K), blue trace (0.38, 0.39; 4200 K). (b) CIE coordinates of corresponding devices plotted on 1931 CIE chromaticity coordinate color space highlighting the CCT for the various devices in the warm-cool white light shade.

chromaticity operating point within the white region of the CIE color space. Here, InP/ZnSe NQDs (λ_{PL}= 570 nm) were used as the green component (Supporting Information Figure S2) and simply mixed with g-NQDs (λ_{PL}= 625 nm; 16-monolayer CdS shell) in different ratios to realize a range of white-light "color temperatures" from cool to warm as a function of the relative contributions of the red, green and blue components (Figure 6). Because g-NQDs exhibit limited self-reabsorption and green absorption, these "traditional" factors do not have to be taken into account when designing color mixtures for a particular white-light characteristic. Therefore, we were able to easily achieve CCTs from 3200 K (warm; relatively more red g-NQD contribution) to 5800 K (cool; relatively more green InP/ZnSe NQD contribution) (Figure 6b).

In conclusion, we have assessed the unique attributes of g-NQDs in the context of down-conversion phosphors for SSL. The key properties distinguishing g-NQDs from conventional NQDs include their enhanced stability and minimal self-reabsorption or unwanted yellow/green absorption, the latter resulting from a characteristic large Stokes shift. As an additional manifestation of their ultrathick shell structure, g-NQDs afford efficient blue-light absorption through their protective shell combined with efficient single-color, narrow-band red emission from the NQD core. Their large Stokes shift cannot by "mimicked" by a mixed NQD (CdSe and CdS) system, as the NQD→NQD (CdS→CdSe) energy transfer process is less efficient than the internal shell→core energy relaxation process, and also results in contributions to PL from CdS excitonic and trap emission. Lastly, the absence of significant yellow/green absorption by red-emitting g-NQDs allows facile fabrication of white-emitting devices in a range of CCT values by simple mixing with green InP/ZnSe NQDs. Future studies are needed to optimize down-conversion devices comprising g-NQD phosphors and, significantly, to fully interrogate the robustness of g-NQDs as color-converting materials at relevant, elevated temperatures (≥85 °C) and high excitation fluxes.

■ ASSOCIATED CONTENT

Ⓢ Supporting Information

Device fabrication details and schematic; NQD synthetic methods; additional film and device absorption and emission spectra; concentrations of active species utilized for device fabrications. This material is available free of charge via the Internet at http://pubs.acs.org.

■ AUTHOR INFORMATION

Corresponding Author

*E-mail: jenn@lanl.gov.

Notes

The authors declare no competing financial interest.

■ ACKNOWLEDGMENTS

Y.G. and H.H. acknowledge support by the Los Alamos National Laboratory Directed Research and Development (LDRD) Program. A.M.D and J.A.H. acknowledge a Single Investigator Small Group Research Grant (2009LANL1096), Office of Basic Energy Sciences (OBES), Office of Science (OS), U.S. Department of Energy (DOE). J.K. is supported in part by a Center for Integrated Nanotechnologies (CINT) postdoctoral research award. This work was performed at CINT, a U.S. DOE, OBES nanoscale science research center and user facility.

■ REFERENCES

(1) Tsao, J. Y. Light Emitting Diodes (LEDs) for General Illumination: An OIDA technology roadmap update 2002, Optoelectronics Industry Development Association (OIDA), Washington, DC; see http://lighting.sandia.gov/lightingdocs/OIDA_SSL_LED_Roadmap_Full.pdf.

(2) Phillips, J. M.; Coltrin, M. E.; Crawford, M. H.; Fischer, A. J.; Krames, M. R.; Mueller-Mach, R.; Mueller, G. O.; Ohno, Y.; Rohwer, L. E. S.; Simmons, J. A.; Tsao, J. Y. *Laser Photon. Rev.* **2007**, *1* (4), 307−333.

(3) DOE EERE Solid-State Lighting Research and Development: Multi Year Program Plan March 2011; see http://www1.eere.energy.gov/buildings/ssl/techroadmaps.html.

(4) Smet, P. F.; Parmentier, A. B.; Poelman, D. *J. Electrochem. Soc.* **2011**, *158* (6), R37−R54.

(5) Yen, W. M.; Shionoya, S.; Yamamoto, H. *Phosphor Handbook*; CRC Press: New York, 2007.

(6) Murray, C. B.; Norris, D. J.; Bawendi, M. G. *J. Am. Chem. Soc.* **1993**, *115* (19), 8706−8715.

(7) Jang, H. S.; Yang, H.; Kim, S. W.; Han, J. Y.; Lee, S. G.; Jeon, D. Y. *Adv. Mater.* **2008**, *20* (14), 2696−2702.

(8) Jang, E.; Jun, S.; Jang, H.; Lim, J.; Kim, B.; Kim, Y. *Adv. Mater.* **2010**, *22* (28), 3076−3080.
(9) Li, Y.; Rizzo, A.; Cingolani, R.; Gigli, G. *Microchim. Acta.* **2007**, *159*, 207−215.
(10) Panzer, M. J.; Wood, V.; Geyer, S. M.; Bawendi, M. G.; Bulovic, V. *J. Display Technol.* **2010**, *6* (3), 90−93.
(11) Wood, V.; Panzer, M. J.; Chen, J.; Bradley, M. S.; Halpert, J. E.; Bawendi, M. G.; Bulović, V. *Adv. Mater.* **2009**, *21*, 2151−2155.
(12) Lim, J.; Jun, S.; Jang, E.; Baik, H.; Kim, H.; Cho, J. *Adv. Mater.* **2007**, *19* (15), 1927−1932.
(13) Nizamoglu, S.; Zengin, G.; Demir, H. V. *Appl. Phys. Lett.* **2008**, *92*, 031102.
(14) Chung, W.; Park, K.; Yu, H. J.; Kim, J.; Chun, B.-H.; Kim, S. H. *Opt. Mater.* **2010**, *32* (4), 515−521.
(15) Dai, Q. Q.; Duty, C. E.; Hu, M. Z. *Small* **2010**, *6* (15), 1577−1588.
(16) Nazzal, A. Y.; Wang, X.; Qu, L.; Yu, W.; Wang, Y.; Peng, X.; Xiao, M. *J. Phys. Chem. B* **2004**, *108* (18), 5507−5515.
(17) Talapin, D. V.; Mekis, I.; Götzinger, S.; Kornowski, A.; Benson, O.; Weller, H. *J. Phys. Chem. B* **2004**, *108*, 18826−18831.
(18) Chen, Y.; Vela, J.; Htoon, H.; Casson, J. L.; Werder, D. J.; Bussian, D. A.; Klimov, V. I.; Hollingsworth, J. A. *J. Am. Chem. Soc.* **2008**, *130* (15), 5026−5027.
(19) Vela, J.; Htoon, H.; Chen, Y. F.; Park, Y. S.; Ghosh, Y.; Goodwin, P. M.; Werner, J. H.; Wells, N. P.; Casson, J. L.; Hollingsworth, J. A. *J. Biophotonics* **2010**, *3* (10−11), 706−717.
(20) García-Santamaría, F.; Chen, Y.; Vela, J.; Schaller, R. D.; Hollingsworth, J. A.; Klimov, V. I. *Nano Lett.* **2009**, *9* (10), 3482−3488.
(21) Htoon, H.; Malko, A. V.; Bussian, D.; Vela, J.; Chen, Y.; Hollingsworth, J. A.; Klimov, V. I. *Nano Lett.* **2010**, *10* (7), 2401−2407.
(22) Pal, B. N.; Ghosh, Y.; Brovelli, S.; Laocharoensuk, R.; Klimov, V. I.; Hollingsworth, J. A.; Htoon, H. *Nano Lett.* **2012**, *12* (1), 331−336.
(23) Brovelli, S.; Schaller, R. D.; Crooker, S. A.; Garcia-Santamaria, F.; Chen, Y.; Viswanatha, R.; Hollingsworth, J. A.; Htoon, H.; Klimov, V. I. *Nat. Comm.* **2011**, *2*, 280.
(24) Lee, J.; Sundar, V. C.; Heine, J. R.; Bawendi, M. G.; Jensen, K. F. *Adv. Mater.* **2000**, *12* (15), 1102−1105.
(25) Mahler, B.; Spinicelli, P.; Buil, S.; Quelin, X.; Hermier, J.-P.; Dubertret, B. *Proc. SPIE* **2008**, *7189*, 718903.
(26) Woggon, U. *Optical properties of semiconductor quantum dots*; Springer-Verlag: Berlin, 1997.
(27) Crooker, S. A.; Hollingsworth, J. A.; Tretiak, S.; Klimov, V. I. *Phys. Rev. Lett.* **2002**, *89* (18), 186802.
(28) Kagan, C. R.; Murray, C. B.; Nirmal, M.; Bawendi, M. G. *Phys. Rev. Lett.* **1996**, *76* (16), 3043−3043.
(29) Fabian, A.; Rente, T.; Szollosi, J.; Matyus, L.; Jenei, A. *ChemPhysChem* **2010**, *11* (17), 3713−3721.
(30) Murray, C. B.; Kagan, C. R.; Bawendi, M. G. *Annu. Rev. Mater. Sci.* **2000**, *30*, 545−610.
(31) Lakowicz, J. R. *Principles of Fluorescence Spectroscopy*; Kluwer Academic/Plenum: New York, 1999.
(32) Achermann, M.; Petruska, M. A.; Crooker, S. A.; Klimov, V. I. *J. Phys. Chem. B* **2003**, *107* (50), 13782−13787.
(33) Müller, T.; Schrey, F. F.; Strasser, G.; Unterrainer, K. *Appl. Phys. Lett.* **2003**, *83* (17), 3572−3574.
(34) Kurtze, H.; Seebeck, J.; Gartner, P.; Yakovlev, D. R.; Reuter, D.; Wieck, A. D.; Bayer, M.; Jahnke, F. *Phys. Rev. B* **2009**, *80*, 235319.
(35) Inoguchi, T.; Mito, S. *Top. Appl. Phys.* **1977**, *17*, 196.